A Quorum Sensing-Based Regulatory System to Model Bacterial Luminescence

Gundeep Singh

April 28 2019

1 INTRODUCTION

1.1 Background and Hypothesis

Quorum sensing (QS) is a cell-cell bacterial communication mechanism that allows the bacterial species to cooperatively regulate specific gene expressions in response to changes in their local population density. The mechanism was first observed by Hastings and Nealson in 1977, where they used the term 'environmental sensing' to describe the population-dependent regulation of bioluminescence in *Vibrio fischeri*. [1] *V. fischeri* is a Gram-negative rod-shaped bacterium species often found living symbiotically with marine species, predominantly in *Monocentris japonica*, *Cleidopus gloriamaris*, and other squid species. [1]. In Gram-negative bacteria, a single QS process is typically activated by an autoinducer molecule, which is synthesized by each bacterial cell individually at basal level and diffused into the surrounding medium. [2] The level of this autoinducer molecule controls the operation of QS network as an 'on-off' gene expression switch, where expression is suppressed in the off-state and induced in the on-state. [3] Thus the term 'quorum' in QS is used in its most literal sense to denote the fact that the gene expression in a bacterial population is strongly induced only when the 'quorum' threshold requirement is met.

Australian marine biologist Sally James in her paper, *Luminescence Control in the Marine Bacterium Vibrio fischeri: An Analysis of the Dynamics of lux Regulation*, introduced the first formal mathematical model to describe the mechanism of QS. [2] In this paper, James attempted to model the phenotypic on-off switch of bioluminescence in *V. fischeri* using a general chemical kinetics approach of lux regulatory system that controls the production of light in the bacteria. [4] The model developed by James has a deterministic form that describes the intracellular dynamics of QS while keeping the extracellular concentration of the autoinducer molecule as a free parameter. In this paper, we have attempted to reproduce the analysis presented by James to describe the switch-like behavior of bioluminescence in *V. fischeri*. Using James' results, we hypothesize that as dictated by the phenomenon of QS, the behavior of bioluminescence switch is governed by the extra-cellular concentration of signaling molecule, but there also exists a certain regime of metabolic conditions that lead to a single cell to luminesce even in absence of external signalling molecule concentration. These metabolic conditions might not correspond to the normal marine environmental parameters, as the luminescence is only strongly observed in the presence of population density. However, these conditions might be achievable in a lab setting to test the model. For example, many luminescence-up mutations have been applied using transposon mutagenesis to mutate the genes that produce the protein products that interact with each other in the regulatory system, which thereby change the interaction parameters of the system to the values required for a single bacterium cell.[5]

The genetic regulatory network of the lux operon responsible for both the production of the signalling molecule and light-producing luciferase in *V. fischeri* is shown schematically in Fig 1. The autoinducer signalling molecule in *V. fischeri* is N-3-oxo-hexanoyl-L-homoserine lactone, or OHHL and is represented by 'A' in Fig 1. The lux operon is further organized in two operons luxR and luxI, which are transcribed divergently to produce two protein products 'R' and 'I' respectively. Protein product I in *V. fischeri* is the OHHL synthase and thus A acts as an autoinducer which induces its own production. Binding of autoinducer A with protein R produces a complex C, which is a transcription factor that directly activates the lux operon, thus inducing the production of both luxR and luxI proteins. In *V. fischeri*, genes luxC, luxD, luxA, luxB, luxE, luxG (lux CDABEG in Fig 1) are also cotranscribed with luxI gene. [6]

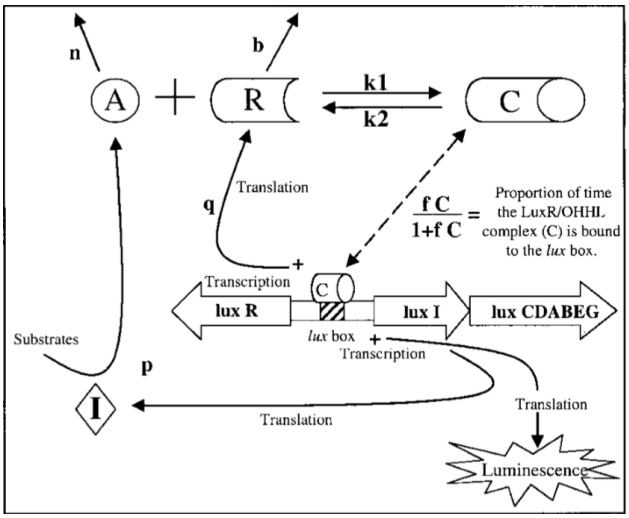

Figure 1: Schematic of lux operon regulatory system. Autoinducer molucule OHHL, denoted by A, binds with protein R to produce complex C. C acts a transcription factor for lux operon and activates the expression of luxR and luxI, which further regenerates autoinducer A and protein product R. Lux CDABEG is coupled to expression of luxI and is responsible for the generation of light in *V. fischeri*[4]

Light is generated by the enzyme luciferase which is composed of products of luxA and luxB, while other genes are responsible for regeneration of other organic compounds necessary for the production of light. [6] Hence, the production of light is directly coupled to the transcription of luxI protein and can be modelled indirectly by the activity of luxI in synthesizing autoinducer A.

1.2 Significance

This research presents a mathematical description of the dynamics of bioluminescence in *V. fischeri* species. The model also describes the environmental and physiological conditions that regulate the production of light in *V. fischeri* in both free and populated states. A key finding of the research is that, even though the overall mechanism of cell-cell communication in *V. fischeri* is through the Quorum Sensing, there exists a certain range of conditions, where a single free marine bacterial cell can also luminesce light, which adds new knowledge to the existing literature of the field.

Bioluminescence in *V. fischeri* is also a model ecological case for studying symbiotic relations in the case when marine organisms act as host to the bacteria. For example, it has been used as a biomedical model for the study of bacterial colonization of animal tissues[7]. The research presented in this paper also sheds light on the ecological aspect of *V. fischeri* by showing the relation between the symbiotic partnership and the population densities of the luminous bacteria.

Quorum sensing is not only employed by *V. fischeri* to control its phenomenon of bioluminescence, but is actually used by a number of bacterial species to control collective bacterial behavior in wide-ranging systems like biofilm formation, competence, motility and virulence. Studying quorum-sensing regulated virulence factor as a quantitative phenomenon, specifically, has its own advantages as there are many human pathogenic bacteria, like Staphylococcus aureus, Bacillus cereus, Pseudomonas aeruginosa, and Vibrio cholerae, that control their virulence factor to launch an enhanced attack inside the human species. [8] Researchers have thus realized the phenomenon of quorum sensing as a target for therapeutics. Quorum-sensing based therapeutics is an active area of study, where the most important technique has been 'Quorum Quenching', first introduced in a 2001 nature paper by Dong et al.[9] Certain bioactive molecules have been systhesized that interrupt the quorum sensing communication pathways and the application of these quorum sensing inhibitors to therapeutics is termed as Quorum Quenching. There is a growing interest for developing quorum sensing-based therapeutic strategies especially for cases where the antibiotic resistance is high since quorum quenching, or other strategies that target virulence pathways do not affect the bacterial growth and

thus face less stringent selection pressures or resistance.[10]

In the final section of this paper, we have extended the James model by introducing the additional parameters in the model that replicate the affect of introducing drugs to the system. We have studied this newer system in correlation with experimental data of inhibition and attempted to find the optimal drug dosage required to most effectively repress the luminescence gene in *V. fischeri*.

2 MODEL DESCRIPTION

Variable	Description
A	Cellular Concentration of the Auto-inducer molecule (ml^{-3})
R	Cellular Concentration of protein product of Lux R (ml^{-3})
C	Cellular Concentration of A and R complex (ml^{-3})

Table 1: State Variables

Parameter	Description	Value
n	Diffusion constant of the auto-inducer A molecule (t^{-1})	10
b	Degradation constant of LuxR protein R (t^{-1})	3
p	Formation of A due to lux gene activity ($ml^{-3}t^{-1}$)	30
q	Formation of R due to lux gene activity ($ml^{-3}t^{-1}$)	5
k_1	Rate constant for binding reaction of A and R to form C ($l^3m^{-1}t^{-1}$)	20
k_2	Rate constant for dissociation of C into A and R (t^{-1})	10
f	Weightage of C that constitutes towards the enhanced activity of lux gene (l^3m^{-1})	1
A_{ex}	Extracellular concentration of auto-inducer A (ml^{-3})	0 or otherwise + const
A_2	Cellular concentration of a secondary auto-inducer (ml^{-3})	0 or otherwise + const

Table 2: Independent Parameters

2.1 Model Equations

2.1.1 Developing the Model

The model is described mathematically by quantifying and mapping the known intracellular interactions of A,R,C and the lux operon as shown in Fig 1. Protein products A and R bind together to form the complex C and this interaction is described by a reversible chemical kinetics equation:

$$\mathrm{A} + \mathrm{R} \underset{k_2}{\overset{k_1}{\rightleftharpoons}} \mathrm{C} \tag{1}$$

$$\text{Formation rate of } C = k_1 AR \tag{2}$$

$$\text{Dissociation rate of } C = k_2 C \tag{3}$$

Complex C is a transcription factor for the lac operon. The activity of lac operon can thus be described by quantifying the proportion of time the complex C is bound to the *lux* box present on the operon, which is described by a Michaelis-Menten type equation:

$$\text{Proportion of time } \textit{lux} \text{ box is occupied} = \frac{fC}{1+fC} \tag{4}$$

Equation (4) says that if the concentration of C is high, such that $fC >> 1$, then the lux box is almost always occupied by the transcription factor and thus does not depend on C. On the other hand if C is small, such that $fC << 1$, then the occupancy proportion is assumed to be linearly dependent of the concentration of C.

As C induces the expression of lux operon, the rate of synthesis of products A and R also increase. However, since the transcription of lux operon is divergent, we consider two constants p and q that describe the rate of formation of A and R respectively:

$$\text{Synthesis rate of } A = p \times \frac{fC}{1+fC} \tag{5}$$

$$\text{Synthesis rate of } R = q \times \frac{fC}{1+fC} \tag{6}$$

Finally, we consider the degradation rates and the diffusion rates of A, R, and C. The model assumes that autoinducer A, OHHL is a highly stable molecule due to the presence of stable lactone ring in the chemical structure. Hence, the dominant decaying rate of A comes from the diffusion of A outside of the bacterium cell in focus. On the contrary, the degradation rate of R is considered dominant over the diffusion rate, due to the presence of active enzymatic breakdown of the protein product. The decaying rate of C is majorly due to the dissociation of the complex back into its constituents, which is already described by rate k_2 in Eq. (3). Thus, putting all the dominant decaying rates of A, R and C together, we get:

$$\text{Diffusion rate of } A = n(A_{\text{eff}}) = n(A - A_{\text{ex}}) \tag{7}$$

$$\text{Degradation rate of } R = bR \tag{8}$$

2.1.2 System Differential Equations

Combining all the rates of change of variables A, R, and C given by the Eq. (1) - (7), we get the following three differential equations that completely describe the system:

$$\frac{dA}{dt} = k_2C - k_1AR - n(A - A_{\text{ex}}) + p\frac{fC}{1+fC} \tag{9}$$

$$\frac{dR}{dt} = k_2C - k_1AR - bR + q\frac{fC}{1+fC} \tag{10}$$

$$\frac{dC}{dt} = k_1AR - k_2C \tag{11}$$

2.1.3 Model Extension : Introducing Quorum Sensing Inhibitors to the System

In our extension, we have used bioluminescence in *V. fischeri* as an analogous system to study virulence factor in population-density dependent pathogens. There are certain species in the system that can be attacked using competitive and non-competitive inhibitors. One of the most common inhibitors of lux regulated quorum sensing are halogenated furanones, which target the turnover of luxR protein product. [11]. The introduction of this drug to our model equation system can be done using the prefactor of (1- ϵ), in the transcription expression of Lux R as done by Anand et al [10]:

$$\frac{dR}{dt} = k_2C - k_1AR - bR + (1-\epsilon) \times q\frac{fC}{1+fC} \tag{12}$$

where $\epsilon \in (0,1)$. ϵ = 0 corresponds to no drug in the system, while ϵ = 1 corresponds to a perfect inhibition of luxR.

2.2 Model Assumptions

1. The stimulation activity of lux operon by the attachment of transcription factor complex C can be modeled by a Michaelis-Menten function.

2. The diffusion rates of R and C are ignored

3. A is considered highly stable under the cellular pH level such that degradation rate of A is also ignored.

4. Activity of lux CDABEG are assumed to be perfectly coupled to lux I, such that transcription of lux I means production of light. This completely ignores the chain of lux genes that are needed to be transcripted in order to ensure luminescence.

5. The intracellular and external concentration of A and A_{ex} are not balanced. That is if intracellular A diffuses out of the cell, then A_{ex}, however there is no balance present in the equations, as A_{ex} is considered to be an independent parameter and not an entity which is similar to A.

2.3 Equilibrium States and Linearization

2.3.1 Equilibrium States

The equilibrium of the system described in Eq. (9)-(11) occurs when the left-hand sides of all three equations are equal to 0. Solving the system of equations results in 3 equilibrium states S_i = (A_i,R_i,C_i) with i = 0,1 and 2. The trivial solution S_0 = (A_{ex},0,0), which correspond to no transcription of lux gene, is the state where there is no luminescence. The other two equilibrium solutions S_1 and S_2 are real when C > $\frac{1}{f}$, as it will be shown in the next section of Results. In this paper, our main goal is to explore the stability conditions for S_1 and S_2. This is necessary as the S_2 state directly correspond to the luminescence state and while S_1 is an essential component that will show the phenotypic switch we hypothesized in the Introduction section.

2.3.2 Linearization

The stability of the 3 equilibrium points are determined by computing the real part of the eigenvalues of Jacobian of the system of ODEs described by Eq. (9)-(11). This is accomplished by taking partial derivatives of Eq (9)-(11) with respect both A, R, and C and estimating their values at each of the three equilibrium points. The eigenvalues of the resulting matrices are then computed to analyze the stability of the equilibrium points. We have used Mathematica's capabilities to work with symbols to analytically determine the Jacobian and the inequalities required for the stability (or instability) of any particular equilibrium points. The results of stability analyses are shown in the next section of Results.

2.4 Numerical Simulation

2.4.1 Figure 3

To numerically explore the stability of the equilibrium point S_2, we ran multiple trajectories from different initial conditions and estimated the time required by each of the trajectory to reach back to the (stable) equilibrium point S_2. The initial conditions were chosen such that they represent concentrations of A, R and C that lie on a surface of a sphere centered at S_2 with a radius of 1 ml^{-3} (see Table 3). To accomplish this in Mathematica, we first created the required sphere as a graphic primitive and then chose random 10,000 points on the surface of the sphere. Taking each of the random surface points as a single initial condition, we solved the ODE system using NDSolve. The solution for every single initial condition thus generated an interpolating function. We computed values of this interpolating function at discrete times from 1 to 100 seconds and estimated the *speed* of approach towards equilibrium, by plugging back the coordinate values into the ODE system. Since the resulting solution is asymptotically symmetrical, we set a cut-off measurement on speed to say such that systems that approach equilibrium with norm of speed < 10^{-3} $ml^{-3}t^{-1}$ are so slow that they have *almost* reached equilibrium. Finally, we created another interpolating function that maps the time required to reach S_2 into a grayscale mapping and used it as a ColorFunction for ListSurfacePlot3D to generate Figure 3.

2.4.2 Figure 4

The technique performed to recreate Fig 4 is very similar to the one used in Fig 3 reconstruction with slight modifications. In this case, we needed to numerically explore the instability of the equilibrium point S_1. Thus, in this case, we computed the time required by the model to end up in either S_0 or S_2. The initial conditions, for this figure

Sphere Center	Sphere Radius
S2 : {A,R,C} = {2.66, 1.48, 7.87} (ml^{-3})	1 (ml^{-3})
S1 : {A,R,C} = {0.34, 0.19, 0.13} (ml^{-3})	0.1 (ml^{-3})

Table 3: Initial Conditions are represented by spherical surfaces centered at equilibrium points S1 and S2

reconstruction, lied on a surface of a sphere centered at S_1 with a radius of 0.1 ml^{-3} (see Table 3). We again ran 100,00 of trajectories corresponding to 10,000 of random surface points using NDSolve, and estimated the speed as being the cutoff parameter to determine the time when the system falls into either S_0 or S_2. The resulting mapping of time values into grayscale function generated the ColorFunction which was employed by ListSurfacePlot3D to generate Fig. 4.

3 RESULTS

3.1 Figure 2 : Steady States of the System

The system of ODEs of bioluminescence in *V. fischeri* described above in 'Model Description' section consists of 3 equations with 3 independent state variables, hence we expect 3 different states in our steady state solution. The equilibrium steady state solution was thus obtained by substituting each of the rates of change (i.e. $\frac{dx}{dt}$) by 0, and solving the resulting system linear system of equations. The first steady state (S_0) is the trivial solution of the system of ODEs and thus always exists, regardless of the parameter values. The other two states (S_1 and S_2) are obtained by solving quadratic roots. Thus, to ensure that S_1 and S_2 states are physically relevant, we obtained the parametric condition such that both S_1 and S_2 are purely real:

$$f > \frac{4bk_2np}{k_1(\mathrm{A_{ex}}n + p)^2q} \tag{13}$$

When external OHHL concentration A_{ex} = 0, the condition reduces to:

$$f > \frac{4bk_2n}{k_1pq} \tag{14}$$

Thus, as long as the above inequality is satisfied by the parameters, the system will have 3 real steady state solutions (see Fig 2). Next we linearized the system using Jacobian Analysis to analyze the stability of the 3 equilibrium points. We obtained the following Jacobian :

$$\begin{bmatrix} -n - \mathrm{k}_1 R & -A\mathrm{k}_1 & \mathrm{k}_2 + \frac{fp}{(\mathrm{C}f+1)^2} \\ -\mathrm{k}_1 R & -b - A\mathrm{k}_1 & \mathrm{k}_2 + \frac{fq}{(\mathrm{C}f+1)^2} \\ \mathrm{k}_1 R & A\mathrm{k}_1 & -\mathrm{k}_2 \end{bmatrix}$$

We computed the eigenvalues of the Jacobian at each of the three steady states:

- S_0: S_0 is trivial solution to the model system of ODEs, S_0 = (A=A_{ex}, R=0, C=0). In our Mathematica Notebook we have shown that all the eigenvalues of S_0 are always negative, as long as all the parameter values are real and positive (i.e. physical). Hence S_0 is always stable. S_0 corresponds to the state of non-luminescence, as the gene activity reduces to basal levels when the system is in state S_0.
- S_1: S_1 is an unstable steady state in the regime of the given parameter values. We obtained 2 eigenvalues of S_1 as positive and 1 as negative, hence overall unstable.
- S_2: S_2 is a stable steady state in the regime of the given parameter values. We obtained all three eigenvalues of S_2 to negative, hence overall stable. The state S_2 corresponds to the state of luminescence, as the gene activity is significantly higher than the basal level at induced state S_2.

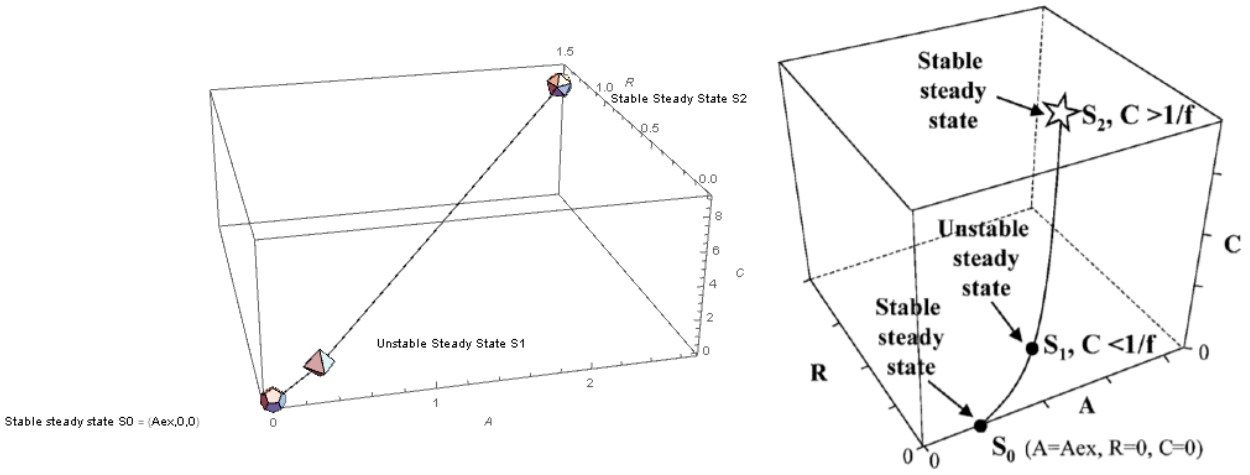

Figure 2: Schematic of three steady state solution of our model's system of ODEs: S_0, S_1, and S_2. S_0 is always stable. S_1 is unstable with the given parameter values. S_2 is stable with the given parameter values. Left: Group Figure. Note that the we used the given parameter values to numerically scale x,y, and z axes and also used $A_{ex} = 0$. Right: Original figure replicated from paper [4]

3.2 Figure 3: Stability of S_2

Since a biological system can exist at a steady state only when there exists a region of local stability around the state to ensure the viability in noisy biological environment, we have analyzed the stability (or instability) of S_2 and S_1 using numerical simulations. The 3-D parameterized graphic with coordinates A vs R vs C shown in Fig 3 demonstrates the local stability around the stable steady state S_2. Each of the points on the spherical surface represents a single initial condition while the corresponding grayscale shading represents the relative time it would take to reach S_2 which lies at the center of the sphere. According to the original paper if, starting from an initial condition point, we reach S_2 in time longer than 15 seconds, then the point is represented by white, while the ones that reach immediately are shaded black. Since S_2 is asymptotically stable, this helped us in determining the minimum threshold on speed we needed to set to obtain the similar scale. We found that a speed of 0.001 (concentration units/sec) produced the required relative scaling of time, and thus grayscale shading.

The diameter of the sphere shown in Fig 3 is equal to 2 conc. units, thus we even go below 1/3rd of equilibrium concentration of R, and we still find that eventually the system will reach S_2. Thus, the main point that Fig 3 conveys is that S_2 has the required local stability to be a biologically relevant state of luminescence, such that if we start from the near vicinity of S_2, the system will reach and sustain the 'on' switch of luminescence.

3.3 Figure 4 : Phenotypic Switch at S_1

Fig 4 is also produced in a similar way as Fig 3, but is now centered around the unstable steady state S_1. The shading is also done similarly to Fig 3, but it now indicates the instability of S_1. Starting from a point lying on the sphere centered around S_1, if system reaches to either of the stable steady states S_0 or S_2 instantaneously, then it is shaded black, and if it takes longer than 15 seconds to reach S_0 or S_2, then it is shaded white. The resulting figure Fig 4 is completely different from Fig 3. In Fig 4, there exists almost a two-shaded surface, where one-half is shaded white and the other is black. The black side mainly correspond to the collapse to trivial steady state S_0, as we know from Fig 3. that it generally takes much longer than 15 seconds to reach S_2 if we are in the nearby region of S_2. Thus, the dark shaded points correspond to rapid collapse of the concentrations to non-luminescent S_0 state, while the bright regions correspond to slow build-up towards luminescence.

3.3.1 Hypothesis Verification

Fig 4 is the key to understand how the model supports our hypothesis: We earlier hypothesized that beside the control of luminescence by extra-cellular concentration of signaling molecule, there also exists a parametric regime where a single cell can act like a QS-mediated luminescence switch even in absence of external signalling molecule.

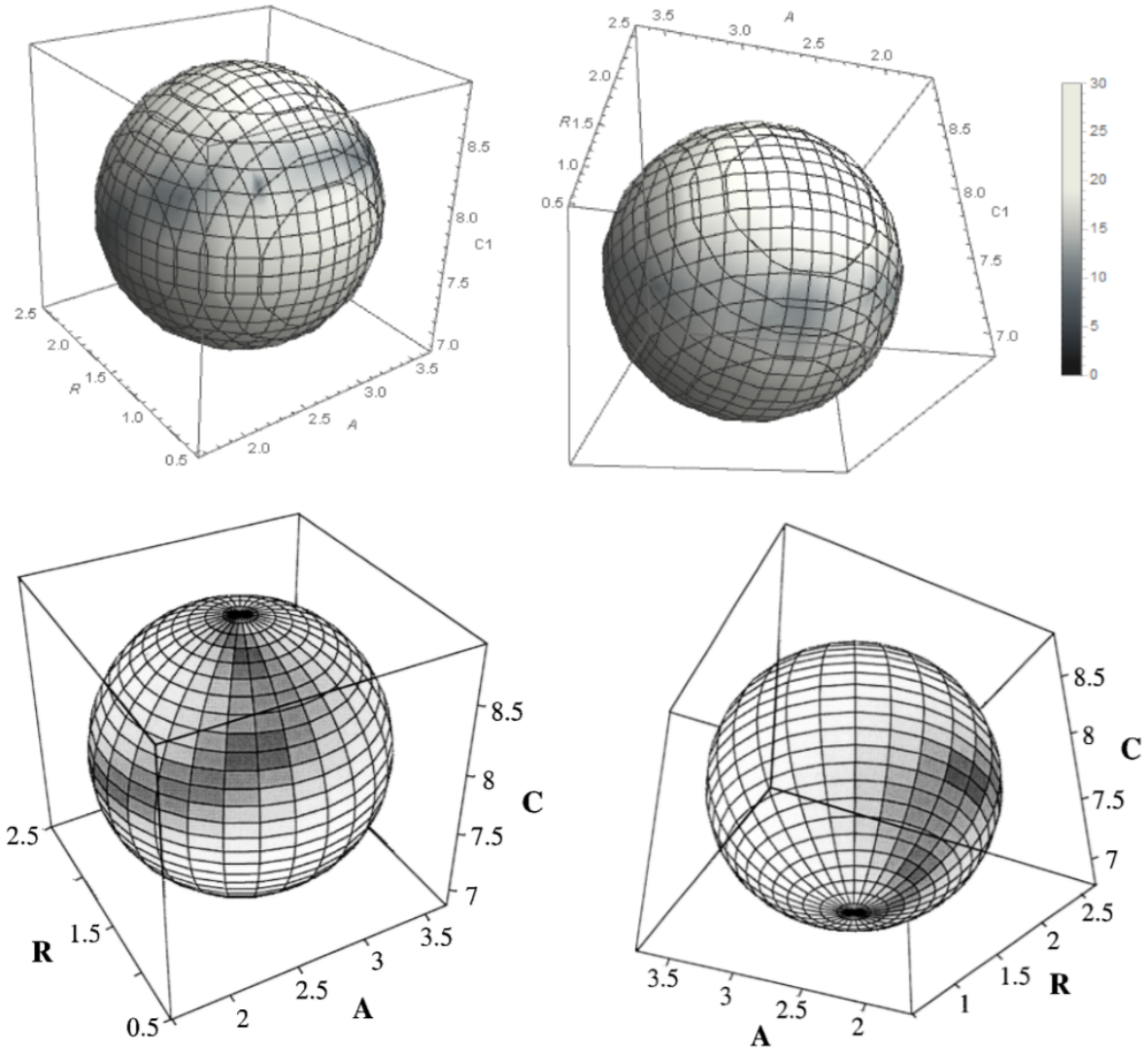

Figure 3: Schematic to demonstrate the stability of S_2, which lies at the center of sphere. Local stability is analyzed away from the center with radius 1 concentration units. Top : Group Figure - Shading scale is shown as a legend, where the numbers correspond the time it takes for the system to asymptotically reach S_2, i.e. when the speed is less than 0.001 conc/sec. Bottom: Original figure replicated from paper. Points are shaded white if they reach to equilibrium in 15 sec or longer and black if they reach immediately. [4]

Fig 4 shows that there is a switch-like behavior of the lux system, where the gene will get turned-on when a certain parametric threshold is achieved. And since the collapse to non-luminescent state S_0 is much faster compared to the slower growth or reach toward S_2, unless the species concentrations of A, R and C are higher than the threshold, there is a chance that the biological noise can rapidly cause the system to converge to the steady state S_0. And all of this is happening in the case when there is no extracellular concentration of OHHL (A_{ex} = 0). Next we will show how the model also supports the facet that we typically expect as a result of Quorum Sensing (QS), that higher the extracellular autoinducer concentration, the chances of reaching S_2 also become higher.

3.4 Figure 5 : In the presence of Extracellular Concentration of OHHL

Inequality (1) introduced in section 1 of Results, required to be satisfied for the existence of biologically relevant steady states S_1 and S_2, can be rearranged to the following:

$$\frac{k_1 pqf}{4bk_2 n} > \left(\frac{1}{1+\frac{n\mathrm{A_{ex}}}{p}}\right)^2 \tag{15}$$

The left hand side of the above inequality is simply the ratio of the products of parameters that increase the cell's ability to have real steady states S_1 and S_2 to the parameters that do the opposite. Fig 4 shows a plot with y axis = k_1pqf, and x-axis = $4bk_2n$ and highlights the region where non-trivial steady states exist, which include S_2, the "on" mode of bio-luminescence. If A_{ex} = 0 then the upper region of the y=x plot will represent the required condition as shown in Fig 5. As it can be seen from Fig 5 or mathematically from Inequality (3), as we increase A_{ex} from 0 to some non-zero positive value, the filled region area expands. This correspond to the relative relaxation of conditions required for existence of S_1 and S_2.

3.5 Discrepancies

- Fig 2 and 3 reproduced using Mathematica are not exactly similar to the ones originally published in the paper. The plausible reason for this discrepancy is that we needed to make our own judgments regarding when can we say that the system has reached equilibrium. Since a system of ODEs produce only asymptotically stable steady state, we needed to set a threshold on speed of apprach or distance from equilibrium point to obtain the times when we can say that the system has "reached" an equilibrium point.

- However it is important to note that our figures still produce the similar overall results presented by James et al [4]. Since the overall picture is relative, the specific shading should not dictate the accuracy of the results. Our figures support both our hypothesis and replicate all of the major results published in [4].

3.6 Model Extension: Results of how Halogenated Furanones affect the model

After, changing the rate of change of R equation Eq. (10) to Eq. (13) after the addition of the drug to the system, we reanalyzed the existence of S_0, S_1 and S_2 and their stability as we increased ϵ from 0 to 1. We found that the system continues to have three steady states S_0, S_1 and S_2 as long as $\epsilon < 0.6$. Thus, $\epsilon = 0.6$ is a saddle-node bifurcation point of the system. We then created the S_1 and S_2 stability spheres like Fig. 3 and Fig. 4. The results are shown in Fig. 6. As it can be seen from the Fig 6, stability of S_2 remain about the same as we increase ϵ from 0 to 0.6, and only starts to weaken as $\epsilon \approx 0.55$. Similar results can be seen in the stability figures of S_1, where the 'on-off' switch remains present as we increase ϵ.

We then studied the affect of the drug to the gene expression levels. These levels are generally reported in the experimental papers, using the intensity expression of light as shown in Fig 3 of [11], which is replicated below as Fig. 7 of this paper. We estimated the data from the white and gray barplots from Fig 7 as two different datasets. We then normalized the fluorescence from 0 to 1, where each run starts from 1 when furanone drug conc. = 0. We also normalized the x-axis linearly, such that the fluorescence concentration corresponds to $\epsilon = 0$ where there is no drug and $\epsilon = 0.6$ (bifurcation point) where the drug is working at its full potential to inhibit the gene expression.

The intensity of fluorescence in our model is non-linearly correlated with the steady state S_2 concentration of C, as C is the the transcription factor which binds to lux box to induce the transcription of lux CDABEG, which leads to the production of light. We modelled this non-linear correlation of with light intensity as an exponential

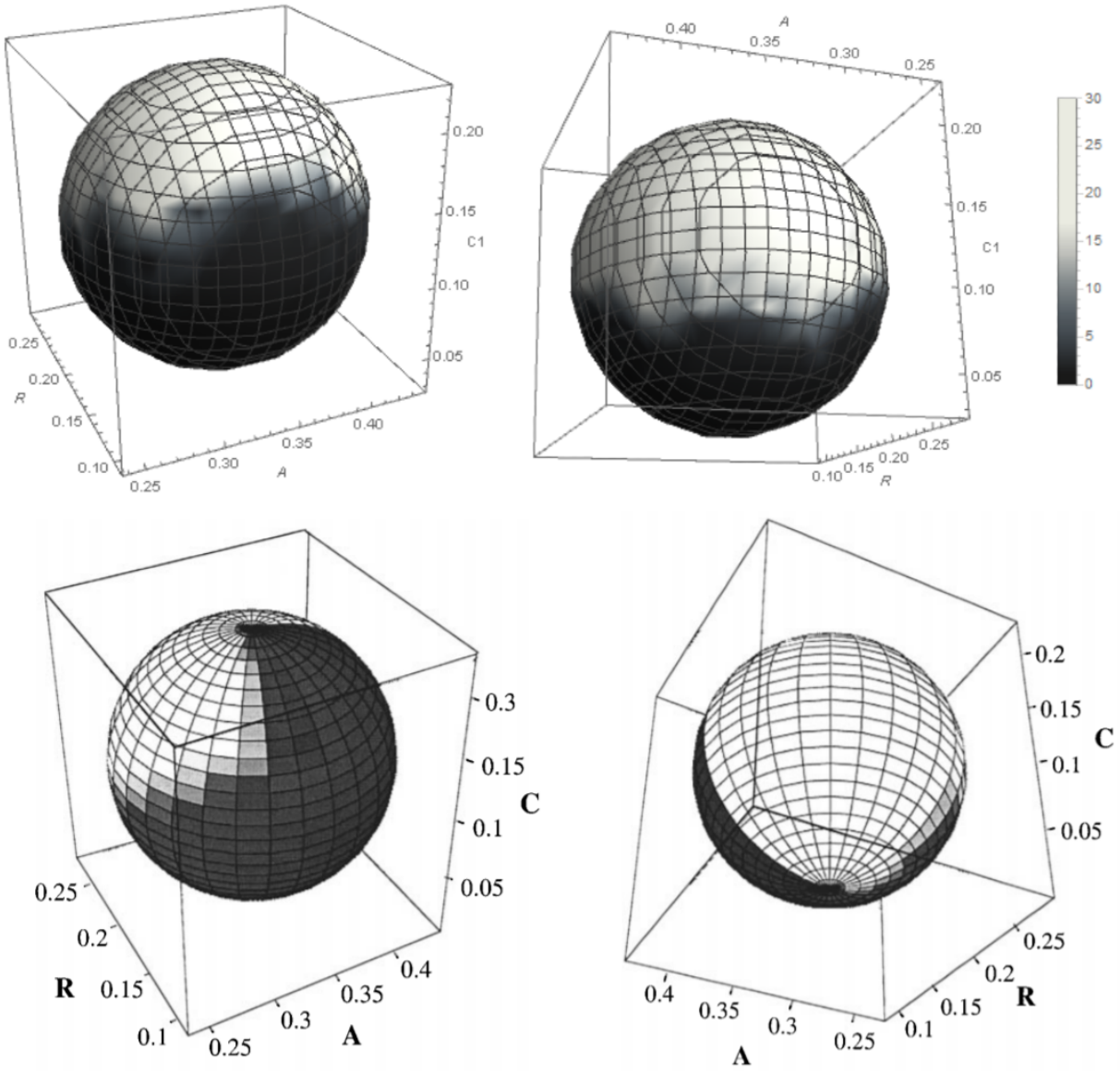

Figure 4: Schematic to demonstrate the instability of S_1, which lies at the center of sphere. Instability is analyzed away from the center with radius 0.1 concentration units. Top : Group Figure - Shading scale is shown as a legend, where the numbers correspond the time it takes for the system to asymptotically reach either of the two stable steady states S_0 or S_2, i.e. when the speed is less than 0.047 conc/sec. Bottom: Original figure replicated from paper. Points are shaded white if they reach to S_0 or S_2 in 15 sec or longer and black if they reach immediately. [4]

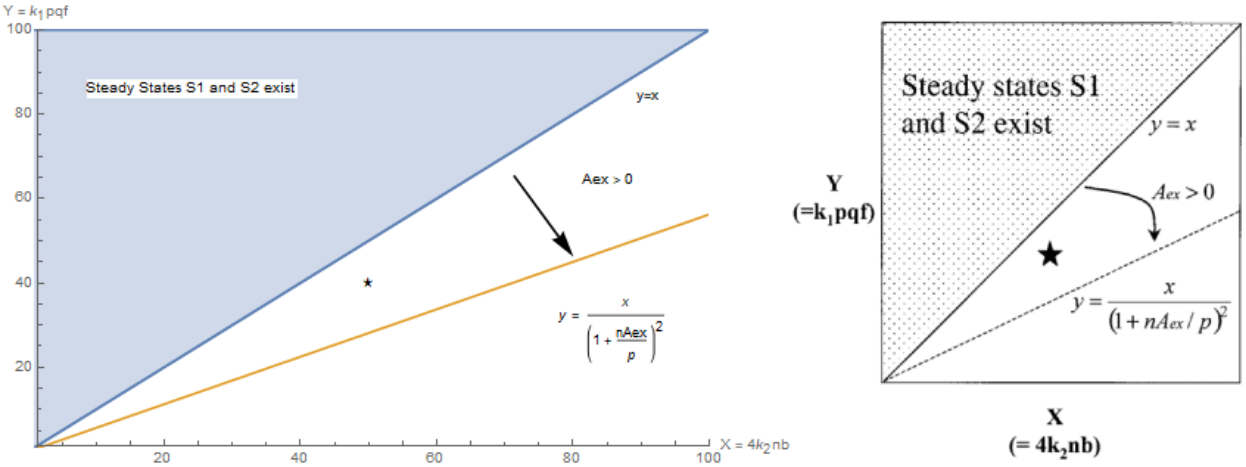

Figure 5: Schematic of the influence of extracellular OHHL on the relaxation of parametric conditions required for the existence of no-trivial steady states S_1 and S_2. When $A_{ex} = 0$, then condition is simply given by y>x. Increasing the A_{ex} to some positive value results in the expansion of parametric area, represented by $\star$. Left : Group figure. Right: Original figure replicated from paper [4]

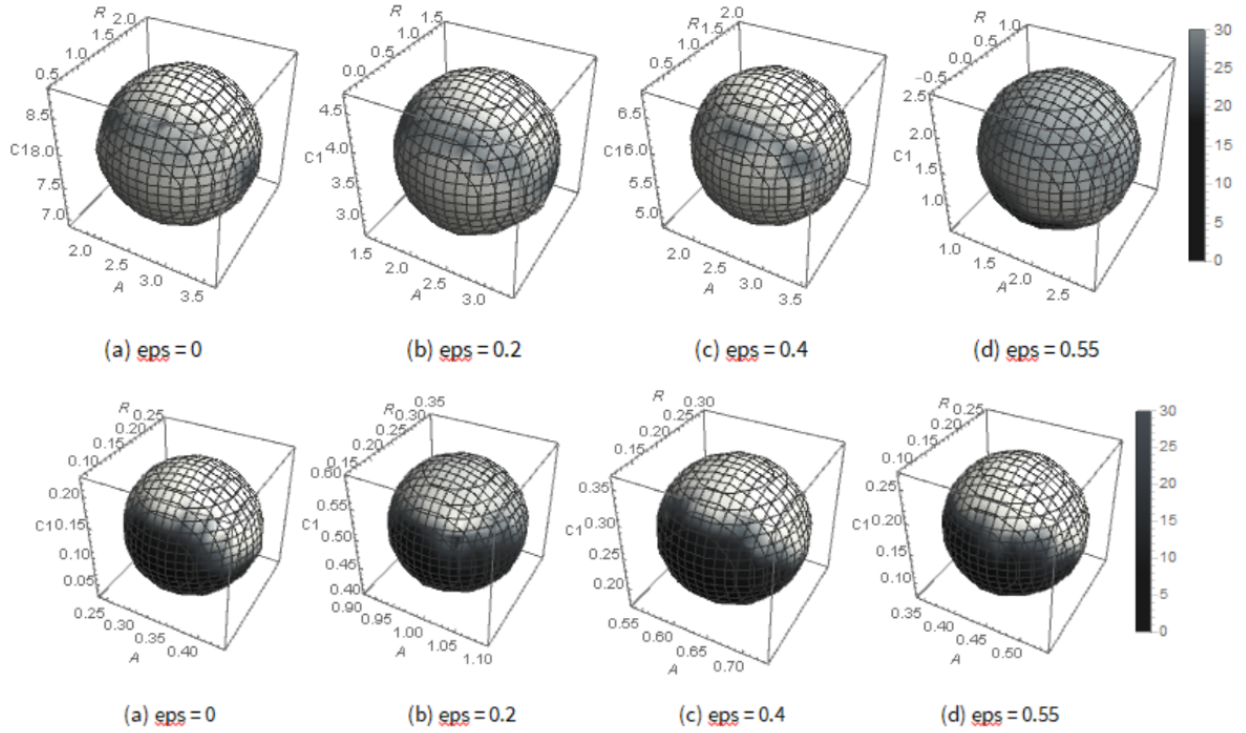

Figure 6: Top: Stability spheres of S_2 of the system as ϵ increases from 0 to 0.6, drawn similarly to Fig.3 . Bottom: Instability spheres of S_1 of the system as ϵ increases from 0 to 0.6, drawn similarly to Fig. 4

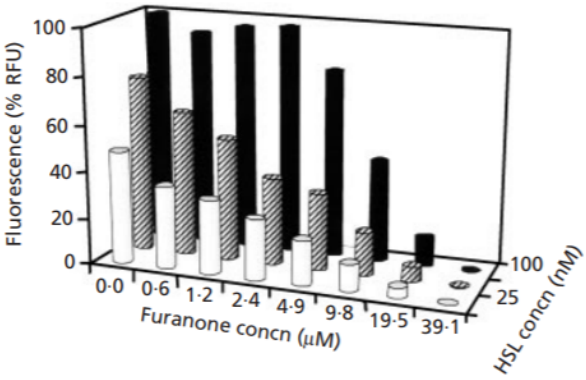

Figure 7: Experimental data of the effect of inhibition of LuxR using halogenated furanones. Intensity of fluorescence (y axis) is plotted against eight different concentrations of furanone (x axis). The z-axis shows the different concentrations of HSL present in the system, which protect the luxR from getting inhibited by halogenated furanones. But for us it just serves as additional data sets. The x- and y-axis data was obtained by eyeballing the plot's different data points. Reproduced from [11]

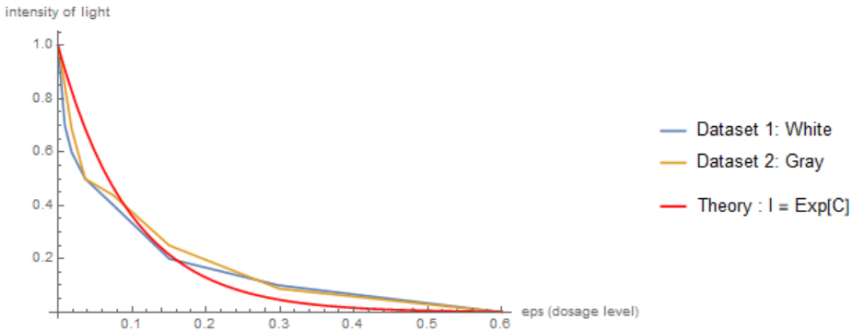

Figure 8: Plot to show the agreement of our theoretical result of the inhibition of luxR with halogenated furanones with the experimental datasets. Dataset 1 and 2 correspond to the normalized data obtained from white and gray barplots respectively. The red curve corresponds to the theoretical estimation of Exp(C) as a function of ϵ at the given parameter values of the system.

as we hypothesize that the change in intensity of light is directly dependent on the light's intensity itself. Thus the attenuation of light follows an exponential decay type relation with C. We found a fantastic agreement to this hypothesis, as after normalizing exp(C) expression, we found it to be a very close alignement with the dataset from Fig 7. This result is is shown in Fig 8.

Finally, we introduced another drug to the system, AHL lactonase which breaks down the autoinducer molecule OHHL, thus causing the downregulation of quorum-sensing based gene expression. So now we have two drugs (ϵ_R and ϵ_A), and our new system equations are :

$$\frac{dA}{dt} = k_2 C - k_1 AR - n(A - A_{\text{ex}}) + (1 - \epsilon_A) \times p\frac{fC}{1 + fC} \tag{16}$$

$$\frac{dR}{dt} = k_2 C - k_1 AR - bR + (1 - \epsilon_R) \times q\frac{fC}{1 + fC} \tag{17}$$

$$\frac{dC}{dt} = k_1 AR - k_2 C \tag{18}$$

With the goal of optimally reducing the concentration of C in the most effective manner, we use Mathematica's minimize operation on the steady state S_2 concentration of C^* as a function of ϵ_R and ϵ_A. We find that with the given

parameter values, there does not exist a sharp minimum in ϵ_R vs ϵ_A vs C*. However, there are certain values, where the repression is slightly more enhanced than other areas and one such point lies at (ϵ_A, ϵ_R) = (epsA -> 0.367448, epsR -> 0.332703).

4 DISCUSSION

4.1 Hypothesis Analysis

Our model results show the switch-like behavior of the bioluminescence we hypothesized in our introduction. The behavior and threshold of this switch is controlled by the model parameter values, where the gene will get turned 'on' once the parameter threshold is achieved. We divided our analysis in two parts - an isolated bacterium cell and a cell in the presence of external autoinducer concentration OHHL diffusing into the cell. A big advantage of such analysis is that we were able to analyze the presence of switch in the absence of external cellular population - i.e. in the absence of 'quorum sensing'. In this case of an isolated cell, we found that there exists a certain regime of parameter values where the bacterium cell can luminesce even at the basal levels of regulatory gene expression. Once we introduce the external population, we see that the parameter conditions become relaxed as shown in Fig 5. Thus, as we expect from the foundational understanding of the mechanism of quorum sensing, once the concentration of A = $A_{ext} + A_{int}$ reaches the threshold (defined by parameter values), the bacterial population enters into the 'on' state of luminescence. This switch-like behavior, the hallmark of quorum sensing has been observed in experiments which analyze the expression of gene with the change in autoinducer concentration (see fig 1B of [12]). Our model, thus successfully capture this switch-like behavior of quorum sensing. But it also highlights an important feature about the activity of gene expression for a bacteria in free state. Since the external autoinducer molecule was modeled such that increasing autoinducer concentration affects the system only by relaxing requirement for steady state solution, we have shown that there might already exist a parametric regime where the cell can luminesce even in free state, and thus not require the 'quorum' condition to be met. But certain parameter values have been selected by the environment, so that an effective external cell-cell communication and collective bacterial behavior is observed and controllable.

4.2 Repressing Bioluminescence using Drugs

Here we have showed how different inhibitory drugs can be modelled into our system to study their affect on the overall gene activity. While there is no immediate significance to our capability to repress luminescence, however a number of different pathogenic bacterial species also use lux gene system to control the production of virulence factor. [13] Thus, our capability to be able to exploit this external communication system and find an optimal target and strategy can help us develop alternate therapeutics, which will be under lower evolutionary resistance as they would not target the bacterial growth.

In this paper, we first introduced Halogenated furanones, a drug the targets luxR turnover. We found that our result matched very well with the experimental data, without any requirement for fitting, thus it confirmed the parameter values used in this paper. We hypothesized that the gene expression or the intensity of light produced is exponentially related to the concentration of the complex C. Thus, the match between theory and experimental data also supports that hypothesis.

Finally, even though, we did not find a sharp dip when using two different drugs in combination, we did find that the two drugs can work together to decrease the gene expression much more effectively than an individual drug. This can be helpful, when we can not give a species high dosage of drugs for safety reasons. In this case, we can give smaller dosages of two or more drugs and still be able to observe the repression of genes.

4.3 Discrepancy

One of the most noticeable discrepancy in our result figures and those published in the original paper, is that the shading is not completely identical in the two [4]. The main reason for this discrepancy, as explained in the result section, is that the scaling of the time the system takes to "reach" the equilibrium state is relative. However, despite the non-uniformity, our figures do provide the same conclusions as those discussed in the paper. Fig. 3 shows that the 'on' state S2 is stable enough that is takes 15 seconds or more for the points at the radius 1 concentration apart to reach S2. On the other hand, Fig. 4 shows the sudden switch-like behavior of the unstable steady state of S1,

where low expression levels of A, R, and C lead the system to rapid collapse to 'off' state, while if the system has crossed the threshold parameter values, the concentration of A_{ex} will grow and take the system to the 'on' state of luminescence.

4.4 Limitations

Our model is only biologically relevant as long as the concentration of A_{ex} is 'not too high', as it gives negative values of state state concentration at 'high' levels of A_{ex}. This assumption made by the original paper goes completely against the notion of quorum sensing, where the behavior of the 'on' state should be supported further as the external concentration of autoinducer molecule is increased.

After this model was published in 2000, a second gene regulatory network of *ain* was discovered that was found to co-regulate the switch of bioluminescence in *V. fischeri*. [14] Thus the two systems of *ain* and *lux* simultaneously regulate the behavior of quorum sensing, and our current model fails to capture the affect of *ain* system to the bioluminescence switch.

4.5 Future Study

A potential study for future would be to integrate the *ain* regulatory network and analyze how the two gene systems co-jointly regulate the switch-like behavior of bioluminescence in quorum sensing.

However, an interesting future study that can test our results of a single bacterium cell being able to luminesce in certain parametric condition, can be to study the luminescence-up mutations. Studies have categorized a number of such mutations, which increase the interaction rates of protein products involved in the gene regulatory system of bioluminescence, thus it would be interesting to see if those mutations actually take us mathematically to the regime where a single cell is able to produce significant light by staying in the the S_2 state. [5]

References

[1] Hastings, J. W. & Nealson, K. H. (1977). Bacterial Bioluminescence *Annual Review of Microbiology, 31*, Pages 549-595.

[2] Pérez-Velázquez, J., Gölgeli, M. & García-Contreras, S. (2016) Mathematical Modelling of Bacterial Quorum Sensing: A Review, *R. Bull Math Biol, 78* (1585), Pages 1-9.

[3] Goryachev, A.B. and Toh, D.J. & Lee, T., (2006). Systems analysis of a quorum sensing network: Design constraints imposed by the functional requirements, network topology and kinetic constants *Biosystems 83* (2), Pages 178 - 187.

[4] James, S., Nilsson, P., James, G., Kjelleberg, S. & Fagerström, T. (2000) Luminescence control in the marine bacterium Vibrio fischeri: an analysis of the dynamics of lux regulation, *Journal of Molecular Biology, 296* (4), Pages 1127-1137.

[5] Lyell, N. L., Dunn, A. K., Bose, J. L. & Stabb, E. V., (2010). Bright Mutants of Vibrio fischeri ES114 Reveal Conditions and Regulators That Control Bioluminescence and Expression of the lux Operon *Journal of Bacteriology 192* (19), Pages 5103-5114.

[6] Stabb, E. (2005). Shedding light on the bioluminescence "paradox" *ASM News 71* (5), Pages 223–229.

[7] Ruby, Edward G., (1999). The Euprymna scolope -Vibrio fischeri Symbiosis: A Biomedical Model for the Study of Bacterial Colonization of Animal Tissue *Journal of Molecular Microbiology and Biotechnology 1* (1), Pages 13-21.

[8] Rutherford, S. T., & Bassler, B. L. (2012). Bacterial quorum sensing: its role in virulence and possibilities for its control. *Cold Spring Harbor perspectives in medicine, 2* (11).

[9] Dong et al. (2001). Quenching quorum-sensing-dependent bacterial infection by an N-acyl homoserine lactonase *Nature, 411*, Pages 813–817.

[10] Anand, R., Rai, N. & Thattai, M. (2013). Interactions among Quorum Sensing Inhibitors *PLOS ONE, 8* (4), Pages 1-10.

[11] Manefield, M., Rasmussen, T., Henzter, M., Andersen, J., Steinberg, P., Kjelleberg, S. & Givskov, M. Halogenated furanones inhibit quorum sensing through accelerated LuxR turnover *Microbiology 148* (4).

[12] Pérez, P. & Hagen, S. (2010) Heterogeneous Response to a Quorum-Sensing Signal in the Luminescence of Individual Vibrio fischeri, *PLOS ONE, 5* (11), Pages 1-9.

[13] Koch B., Liljefors T., Persson T., Nielsen J., Kjelleberg S. & Givskov M. The LuxR receptor: the sites of interaction with quorum-sensing signals and inhibitors *Scientific Reports 7* (1).

[14] Lupp, C., & Ruby, E. G. (2005). Vibrio fischeri uses two quorum-sensing systems for the regulation of early and late colonization factors. *Journal of bacteriology, 187* (11), Pages 3620–3629.